IEEE Access
Multidisciplinary | Rapid Review | Open Access Journal

Received August 5, 2019, accepted August 17, 2019, date of publication August 27, 2019, date of current version September 10, 2019.

Digital Object Identifier 10.1109/ACCESS.2019.2937753

Low-Complexity Partial Transmit Sequence Methods Using Dominant Time-Domain Samples for Multicarrier Faster-Than-Nyquist Signaling

BIAO CAI, AIJUN LIU, (Member, IEEE), AND XIAOHU LIANG
College of Communications and Engineering, PLA Army Engineering University, Nanjing 210007, China

Corresponding author: Aijun Liu (liuaj.cn@163.com)

This work was supported in part by the National Science Foundation of China under Grant 61671476, and in part by the Natural Science Foundation of Jiangsu Province of China under Grant BK20180578.

ABSTRACT In Multicarrier faster-than-Nyquist (MFTN) systems, one of the most important problems of MFTN signaling is high peak-to-average power ratio (PAPR). In this paper, partial transmit sequence (PTS) method is adopted to resolve this problem, and we focus on reducing the computational complexity of it. First, the PTS method combined with alternative signal (AS) is introduced to overcome the overlapping structure of MFTN signaling. Then, due to the dominant time-domain samples of MFTN signaling are used, a new metric which can select dominant time-domain samples accurately is proposed. Based on that, two low-complexity PTS methods are proposed. To further reduce the computational complexity, by analyzing the position distribution of sample with peak power, part of the samples are removed from the procedure of calculating metric for selecting dominant time-domain samples. Simulation results confirm that the proposed low-complexity PTS methods can effectively reduce computational complexity without degrading the PAPR reduction performance.

INDEX TERMS Multicarrier faster-than-Nyquist (MFTN), peak-to-average power ratio (PAPR), partial transmit sequence (PTS), dominant time-domain samples.

I. INTRODUCTION

Multicarrier modulations are methods to modulate data on multiple subcarriers in communication systems. Since the high spectral efficiency, they have attracted wide attention in recent years. One of them is multicarrier faster-than-Nyquist (MFTN) [1]. Compared with conventional multicarrier Nyquist modulations, such as orthogonal frequency division multiplexing (OFDM) [2], the time packing in adjacent symbols and frequency packing in adjacent subcarriers allow MFTN to achieve higher spectral efficiency [3]. Therefore, it has attracted wide interests in future satellite and optical communication systems [4]–[6].

The idea of single carrier faster-than-Nyquist (FTN) can be dated back to 1975, when it was first proposed by Mazo in [7]. In his work, he found that binary sinc pulses could be sent faster than Nyquist's limit for orthogonal pulse while keeping the same asymptotic error probability. In 2003, the FTN with root raised cosine (RRC) pulse was investigated in [8]. It was shown that the Mazo limit, the minimum time packing ratio without decreasing the minimum Euclidean distance, is lower than sinc pulse. Then, MFTN was proposed in 2005 [9] by adopting the concept of FTN to both time and frequency domain. Since both time interval between adjacent symbols and frequency spacing between adjacent subcarriers are reduced, the spectral efficiency can be further improved than single carrier case.

However, one of the major drawbacks of MFTN systems is high peak-to-average power ratio (PAPR) in the transmitted signals. It is known that high power amplifier (HPA) is widely used in practical communication systems. Duo to the non-linear property of HPA, the in-band-distortion and out-of-band radiation occur in the HPA output of MFTN signaling with high PAPR, which leads to the degradation of communication quality. An increase in back-off for HPA will lead to a loss in power efficiency, therefore, PAPR reduction is necessary and more efficient.

Unfortunately, since the serious intersymbol interference (ISI) and intercarrier interference (ICI) introduced by time packing and frequency packing in MFTN signaling,

The associate editor coordinating the review of this article and approving it for publication was Dongxiao Yu.

current researches about MFTN mainly focus on spectral efficiency and signal detection algorithms [10]– [13]. For example, a soft input and soft output (SISO) frequency domain equalization detection algorithm was proposed in [10]. By utilizing the iterative turbo equalization, the ISI and ICI can be effectively eliminated in low complexity. In [11], a maximum signal-to-interference ratio (SIR) scheme was proposed for MFTN systems. Recently, a partial transmit sequence (PTS) based PAPR reduction method has been proposed in [14]. In order to overcome the overlapped structure of adjacent symbols in MFTN signaling and improve the performance of conventional PTS, a two-stage phase rotation was introduced. However, compared with conventional PTS, the complexity of search for finding the optimal two-stage rotation phase factors and the overhead of side-information are too high. Therefore, the PAPR reduction method in [14] is not so attractive.

On the other hand, the PAPR reduction has been widely investigated in OFDM systems. Specifically, duo to the high computational complexity of conventional PTS method, various kind of low-complexity PTS methods were proposed. In [15]–[18], the intelligence algorithms are utilized to find the optimal phase rotation vector. In [19]–[21], the replication computations of conventional PTS method are removed to reduce the computational complexity. In [22]–[24], sub-optimal searching algorithms are adopted to reduce the search complexity. In [25], these PTS methods are analytically reviewed and well summarized. Among them, one of the most attractive methods is using dominant time-domain samples [26]–[29]. The key idea is that using metrics to estimate the amplitude upper bounds of samples among all candidate signal sequences for each index, and selecting dominant time-domain samples in accordance with upper bounds, then, only the dominant time-domain samples are used to estimate the PAPR of each candidate signal sequence. It is noteworthy that none of the metrics in [26]–[29] can estimate the achievable upper bounds accurately.

Regarding these issues, we investigate the PAPR reduction of MFTN signaling based on PTS method in this paper. First, we briefly describe the MFTN signaling, and refine the PAPR of MFTN signaling under a given time and frequency packing ratio. Then, a conventional PTS method is introduced and applied to MFTN signaling.

1) After that, in order to overcome the overlapped structure of MFTN signaling, PTS method combined with alternative signal (AS) [30] is proposed.
2) And, we propose a new metric which can select dominant time-domain samples accurately.
3) Based on that, two low-complexity PTS methods with fixed and fluctuant threshold are proposed.
4) Then, we analyze the position distribution of sample with peak power, and remove part of samples from the procedure of calculating the metric for selecting dominant time-domain samples based on the analysis.

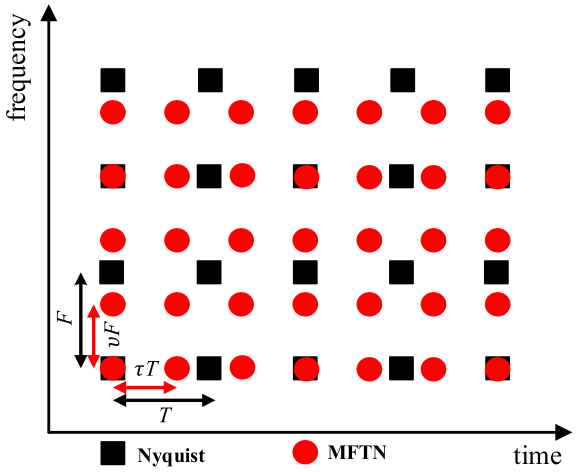

FIGURE 1. The time-frequency grid of MFTN signaling.

It is worthy of note that 2), 3) and 4) are the main contributions of this paper. The proposed low-complexity PTS methods can achieve much lower computational complexity without degrading the PAPR reduction performance.

The rest of this paper is organized as follows. Section II gives the expression of MFTN signaling and refines PAPR definition. Section III describes the conventional PTS and PTS combined with AS (PTS-AS) in MFTN signaling. Then, a new metric for selecting dominant time-domain samples, and two low-complexity PTS methods are proposed in section IV. In section V, the position distribution of sample with peak power is analyzed and part of samples are removed from the calculation of metric to further reduce the computational complexity. After that, computational complexity of proposed methods and simulation results are given in section VI. Section VII is the conclusion.

II. MFTN SIGNALING AND PAPR

Consider a baseband MFTN signaling adopting quadrature phase shift keying (QPSK) with K subcarriers. The independent and identical distributed (i.i.d) information symbol $x_{l,k}$ where l is time index and k is subcarrier index, passes through baseband shaping filter with shaping pulse $g(t)$. Then, by combining the shaped signal and its time-frequency shifted versions with different pairs of (l, k), we can arrive at the baseband MFTN signaling which is given by

$$s(t) = \sum_{l=0}^{+\infty} \sum_{k=0}^{K-1} x_{l,k} g(t - l\tau T) e^{j2\pi k \upsilon F (t - l\tau T)} \quad (1)$$

where $g(t)$ is baseband shaping pulse assumed to have unit energy, that is, $\int_{-\infty}^{+\infty} |g(t)|^2 dt = 1$. Fig. 1 shows the time-frequency grid of MFTN signaling. Generally, $g(t)$ is T-orthogonal shaping pulse in conventional multicarrier Nyquist systems, which means that $\int_{-\infty}^{+\infty} g(t - lT) g(t - mT) dt = 0, l \neq m$. And F is the minimum orthogonal frequency spacing between adjacent subcarriers. For example, $F = 1/T$ for sinc pulse,

and $F = (1+\beta)/T$ for RRC pulse with roll-off factor β. In MFTN signaling, the packed time interval and packed frequency spacing are $\tau T \leq T$ and $\upsilon F \leq F$, respectively, therefore, the time and frequency packing factors $\tau, \upsilon \in (0, 1]$. And, it will be the conventional multicarrier Nyquist communication system when $\tau \cdot \upsilon = 1$.

The PAPR is a convenient parameter that commonly used in measuring the fluctuation degree of the transmitted signal with non-constant envelope. Similar to general multicarrier transmission systems, PAPR of MFTN signaling can be still defined in each symbol time interval τT. We divide the MFTN signaling into intervals with equal time duration τT, and arrive at the PAPR in the l-th symbol interval expressed as

$$PAPR_l \triangleq 10\log_{10}\frac{\max\limits_{l\tau T\leq t<(l+1)\tau T}|s(t)|^2}{E\left[|s(t)|^2\right]} \tag{2}$$

where $E[\cdot]$ is the expectation operation.

Complementary cumulative distribution function (CCDF) is adopted here to exhibit the distribution of PAPR. It is defined as the probability that PAPR exceeds a given value $PAPR_0$, i.e.,

$$CCDF = Pr(PAPR > PAPR_0). \tag{3}$$

It is known that PTS method is implemented on discrete time signals. Therefore, we need to transform (1) and (2) into discrete forms. First, we sample the MFTN signaling with time interval T_c' and define $s\left[n'\right] = s(n'T_c')$, and the discrete time MFTN signaling can be obtained by

$$s\left[n'\right] = \sum_{l=0}^{+\infty}\sum_{k=0}^{K-1} x_{l,k}\, g\left[n' - l\tau N'\right] e^{j2\pi\upsilon\frac{k}{K}(n'-l\tau N')}. \tag{4}$$

However, the nonlinear distortions often occur in analog components, and we are more interested in the PAPR of continuous time MFTN signaling. To better approximate the true PAPR of continuous time MFTN signaling, the discrete time MFTN signaling is obtained by oversampling. Similar to conventional multicarrier Nyquist signals, the J times oversampling can be conducted by applying $(J-1)K$ zeros-padding to the l-th data block x_l, i.e.,

$$x_l = [x_{l,0}, x_{l,1}, \cdots, x_{l,K-1}, \underbrace{0, \cdots, 0}_{(J-1)K}]. \tag{5}$$

It has been confirmed in [35] that $J \geq 4$ is sufficient to acquire the accurate PAPR, therefore, $J = 4$ will be adopted in the following parts of the paper.

Then, the sample interval $T_c = T_c'/J$, that is $s[n] = s(nT_c)$, and the oversampled discrete time MFTN signaling can be expressed by

$$s[n] = \sum_{l=0}^{+\infty}\sum_{k=0}^{K-1} x_{l,k}\, g[n - l\tau N]\, e^{j2\pi\upsilon\frac{k}{JK}(n-l\tau N)} \tag{6}$$

in which $g[n]$ is sampled shaping pulse with finite support $\left[-L_g/2, L_g/2\right]$ and $N = JN'$. And the corresponding PAPR is defined by

$$PAPR_l \triangleq 10\log_{10}\frac{\max\limits_{l\tau N\leq n<(l+1)\tau N}|s[n]|^2}{E\left[|s[n]|^2\right]}. \tag{7}$$

III. PAPR REDUCTION WITH PTS AND PTS-AS

A. CONVENTIONAL PTS

In conventional PTS method, the l-th input data block $x_l = \left[x_{l,0}, x_{l,1}, \ldots, x_{l,K-1}\right]$ is partitioned into U disjoint subblocks represented by $\left\{x_l^{(u)}, u = 0, 1, \ldots, U-1\right\}$. Thus, we have

$$x_l = \sum_{u=0}^{U-1} x_l^{(u)} \tag{8}$$

in which $x_l^{(u)} = \left[x_{l,0}^{(u)}, x_{l,1}^{(u)}, \ldots, x_{l,K-1}^{(u)}\right]$ and

$$x_{l,k}^{(u)} = \begin{cases} x_{l,k}, & k \text{ in the } u\text{-th subblock} \\ 0, & \text{otherwise} \end{cases}. \tag{9}$$

There are various categories of subblock partitioning methods [31]–[34]. Among them, the three most common categories are adjacent, interleaving and random partitioning methods [25]. The adjacent method allocates K/U successive symbols to the same subblock. The interleaving method allocates symbols with distance U to the same subblock. The random partitioning method partitions the input data block randomly.

Then, the MFTN symbols in the data subblock $x_l^{(u)}$ are shaped by pulse $g[n]$ to arrive at $x_{l,k}^{(u)} g[n - l\tau N]$. After modulation with corresponding subcarriers, we can acquire

$$\begin{aligned} &x_{l,k}^{(u)} g[n - l\tau N]\, e^{j2\pi\upsilon\frac{k}{JK}(n-l\tau N)}, \\ &\qquad k = 0, 1, \ldots, K-1, \\ &\qquad -L_g/2 + l\tau N \leq n \leq L_g/2 + l\tau N. \end{aligned} \tag{10}$$

Next, by adding all the modulated subcarriers in one subblock, we can acquire the signal subsequences of the l-th MFTN data block by

$$s_l^{(u)}[n] = \sum_{k=0}^{K-1} x_{l,k}^{(u)} g[n - l\tau N]\, e^{j2\pi\upsilon\frac{k}{JK}(n-l\tau N)}. \tag{11}$$

In order to generate the candidate MFTN signal sequences, these signal subsequences are multiplied by independent phase rotation factors $\{b_u, u = 0, 1, \ldots, U-1\}$, where $b_u = e^{j\phi_u}$ [14]. In practical implementation, the values of phase rotation factors are usually fetched from a finite set defined by $b_u \in \left\{e^{j2\pi w/W}, w = 0, 1, \ldots, W-1\right\}$, in which W is the number of all possible phases of phase rotation factors. The phase rotation vectors, composed by U independent phase rotation factors, are defined by $b^c = \left[b_0^c, b_1^c, \ldots, b_{U-1}^c\right]$, $c = 0, 1, \ldots, C-1$, where C is the number of candidate signal sequences to be generated. For a given phase rotation

vector b^c, the corresponding candidate signal sequence is generated by

$$s_l^c[n] = \sum_{u=0}^{U-1} b_u^c s_l^{(u)}[n]. \tag{12}$$

Because the first phase rotation factors of all phase rotation vectors can be fixed to 1, $C = W^{U-1}$. The objective of conventional PTS is to find the optimal candidate signal sequence with lowest peak power for transmission, which is expressed by

$$\min_c \max_{-L_g/2+l\tau N \le n \le L_g/2+l\tau N} \left|s_l^c[n]\right|^2. \tag{13}$$

Since this paper does not focus on the subblock partition scheme and search algorithm, and the number of phase rotation vectors is finite, the adjacent partition scheme and exhaustive search are adopted in conventional PTS and the proposed methods in the rest of the paper.

B. PTS-AS

Due to the overlapped structure of adjacent symbols, the conventional PTS method shows poor performance in PAPR reduction of MFTN signaling [14]. The AS method is first proposed in [30]. In [35], selective mapping (SLM) combined with AS shows good performance in MFTN signaling. In consideration of that fact that both PTS and SLM are based on phase rotation, combining PTS with AS will be a good way to improve the performance effectively. Thus, in this subsection, we propose the PTS-AS method. The procedures of PTS-AS method to generate the candidate signal sequences are same as that of conventional PTS method. For the sake of concision, those procedures are omitted here.

Compared with conventional PTS method, the main difference of PTS-AS method is sequential optimization. The previous MFTN symbols are taken into account when finding the optimal candidate signal sequence of current MFTN data block. And the detailed description is formulated as follows.

For the zero-th MFTN data block, we use the subsequences calculated by (11) to generate all possible candidate signal sequences $s_0^c[n], c = 0, 1, \ldots, C-1$, and choose the one with lowest peak power by

$$\hat{s}_0[n] = \arg\min_c \max_{-L_g/2 \le n \le L_g/2} \left|s_0^c[n]\right|^2. \tag{14}$$

where $\hat{s}_0[n]$ is the chosen signal sequence of zero-th MFTN data block. Then, $\hat{s}_0[n]$ is utilized to find the optimal signal sequence of the first MFTN data block, and the corresponding optimization problem expressed by

$$\hat{s}_1[n] = \arg\min_c \max_{-L_g/2+\tau N \le n \le L_g/2+\tau N} \left|\hat{s}_0[n] + s_1^c[n]\right|^2. \tag{15}$$

By that analogy, $\hat{s}_0[n]$ and $\hat{s}_1[n]$ are utilized to find the new optimal signal sequence $\hat{s}_2[n]$. And the procedure above is repeated in subsequent MFTN symbols. Therefore, the general procedure of PTS-AS method can be formulated by

$$\hat{s}_l[n] = \arg\min_c \max_{-L_g/2+l\tau N \le n \le L_g/2+l\tau N} \left|\sum_{i=0}^{l-1} \hat{s}_i[n] + s_l^c[n]\right|^2. \tag{16}$$

Since the previous MFTN symbols are taken into account, the first phase rotation factor of phase rotation vector can not be fixed. We can see that the number of candidate signal sequences is $C = W^U$ in PTS-AS method, which is more than conventional PTS method. The increase of C means that more candidate signal sequences need to be generated, that is, computational complexity is higher. However, conventional PTS shows poor PAPR reduction performance in MFTN signaling, and complexity reduction can not bring it the performance improvement, which means reducing the complexity of conventional PTS in MFTN signaling is meaningless and an effective PAPR reduction method is necessary here. The proposed PTS-AS in this paper is a good choice and shows good performance in overcoming the overlapped structure in MFTN signaling. In the following parts of the paper, we will focus on reducing the complexity of PTS-AS method in MFTN signaling.

IV. LOW-COMPLEXITY PTS METHODS USING DOMINANT TIME-DOMAIN SAMPLES

It is known that main drawback of conventional PTS method is high computational complexity, and the vast majority of it comes from the generation of all possible candidate MFTN signal sequences [19], [36], [37]. Moreover, the C is larger in PTS-AS method, which results in increase of computational complexity. Thus, reducing the complexity of generating candidate signal sequences is meaningful. One of the good choices is using dominant time-domain samples. The main idea of it is that only a few dominant time-domain samples for each candidate MFTN signal sequence are generated and used to find the optimal phase rotation vector instead of all the time-domain samples. In [26]–[29], several metrics have been proposed to select the dominant time-domain samples. However, none of them can estimate the achievable amplitude upper bounds of samples among all candidate signal sequences accurately.

In this section, we propose a new metric which can estimate the amplitude upper bounds accurately, and give an efficient calculation of the metric by removing the replication computations. After that, two low-complexity PTS methods are proposed by utilizing the new metric. For the convenience of description, LC-PTS1 and LC-PTS2 are used to represent these two PTS methods.

A. THE NEW METRIC

In PTS-AS method, the achievable amplitude upper bound of samples among all candidate MFTN signal sequences for a

$$\left|\max \operatorname{ang}\left\{\sum_{i=0}^{l-1}\hat{s}_i[n], b_0^c s_l^{(0)}[n], \ldots, b_{U-1}^c s_l^{(U-1)}[n]\right\} - \min \operatorname{ang}\left\{\sum_{i=0}^{l-1}\hat{s}_i[n], b_0^c s_l^{(0)}[n], \ldots, b_{U-1}^c s_l^{(U-1)}[n]\right\}\right| \le \frac{2\pi}{W} \quad (19)$$

given index n can be calculated by

$$M_{l,n} = \max_{0\le c\le C-1}\left|\sum_{i=0}^{l-1}\hat{s}_i[n] + s_l^c[n]\right|, \quad -L_g/2 + l\tau N \le n \le L_g/2 + l\tau N \quad (17)$$

where $M_{l,n}$ represents the achievable amplitude upper bound, and l is the index of current MFTN data block. The greater $M_{l,n}$ implies higher probability that the peak power of candidate signal sequences occurs at sample with index n for the l-th MFTN data block. Thus, $M_{l,n}$ is a proper metric to select the dominant time-domain samples. However, it can not be directly used. The calculation in (17) needs to traverse c from 0 to $C-1$, which means that all candidate signal sequences need to be generated. That is, the adoption of $M_{l,n}$ is unable to reduce the computational complexity of generation of candidate signal sequences.

Here, we propose a new metric to estimate $M_{l,n}$. First, we note that the calculation in (17) is actually the addition of $U+1$ complex numbers, i.e.,

$$\sum_{i=0}^{l-1}\hat{s}_i[n], s_l^{(0)}[n], s_l^{(1)}[n], \ldots, s_l^{(U-1)}[n], \quad (18)$$

and the phases of U complex numbers can be rotated. When $M_{l,n}$ is reached, the corresponding complex plane vectors of these $U+1$ numbers will lay in a sector whose angle is not greater than $2\pi/W$. It can be expressed in formulation by (19), as shown at the top of this page in which ang[·] represents the extraction of the phases. According to the analysis, we can rotate all the $U+1$ complex numbers in (18) by rotation factors and make them lay in a sector on the complex plane of which the angle range from 0 to $2\pi/W$. Then, these rotated complex numbers are ranked in ascending order of phases, and the set $\{a_u, u = 0, 1, \cdots U\}$ is employed to represent them for the sake of convenience. After that, we multiply $2\pi/W$ with each element in the set in turn and obtain $U+1$ sets defined by

$$\begin{aligned}
&\{a_0, a_1, \cdots, a_{U-2}, a_{U-1}, a_U\}\\
&\left\{\frac{2\pi}{W}a_0, a_1, \cdots, a_{U-2}, a_{U-1}, a_U\right\}\\
&\left\{\frac{2\pi}{W}a_0, \frac{2\pi}{W}a_1, \cdots, a_{U-2}, a_{U-1}, a_U\right\}\\
&\qquad\vdots\\
&\left\{\frac{2\pi}{W}a_0, \frac{2\pi}{W}a_1, \cdots, \frac{2\pi}{W}a_{U-2}, a_{U-1}, a_U\right\}\\
&\left\{\frac{2\pi}{W}a_0, \frac{2\pi}{W}a_1, \cdots, \frac{2\pi}{W}a_{U-2}, \frac{2\pi}{W}a_{U-1}, a_U\right\}. \quad (20)
\end{aligned}$$

By summing all elements in each set above, for example, $A_0 = a_0 + a_1 + \cdots + a_U$, we can acquire $U+1$ complex numbers represented by $\{A_i, i = 0, 1, \ldots, U\}$. Finally, the new metric $Q_{l,n}$ can be estimated by

$$Q_{l,n} = \max_{0\le i\le U}|A_i|. \quad (21)$$

In addition, there are some replication computations in calculation of $\{A_i, i = 0, 1, \ldots, U\}$ which can be removed to reduce the computational complexity. For example, both A_0 and A_1 need U complex additions expressed by

$$\begin{aligned}
&a_0 + a_1 + \cdots + a_U\\
&\frac{2\pi}{W}a_0 + \underbrace{a_1 + \cdots + a_U}_{\text{replication additions}}
\end{aligned} \quad (22)$$

of which all the additions are superfluous except the first one. Based on the analysis above and the feature of sets in (20), we can acquire the more efficient calculation by

$$A_i = A_{i-1} - a_{i-1} + \frac{2\pi}{W}a_{i-1}, \quad i = 1, 2, \ldots, U. \quad (23)$$

Except for A_0, only one multiplication and two additions are required in the calculation of each A_i. Compared with directly adding all elements, utilizing (23) is more efficient especially for large U.

For easy understanding of the new metric, an example with $U = 4$ and $W = 4$ is exhibited here. First, we acquire 5 complex numbers according to (18), which is shown in Fig. 2(a). Then, all of them are rotated to the first quadrant by rotation factors and ranked in ascending order of phases. Thus, we can acquire $\{a_u, u = 0, 1, \ldots, 4\}$ as shown in Fig. 2(b). Next, we rotate the first 4 of them one by one and Fig. 2(c)-(f) are obtained. Add all the complex numbers in the same subfigure, i.e., Fig. 2(b)-(f), we can obtain $\{A_i, i = 0, 1, \ldots, 4\}$. Finally, we can arrive at the new metric by substituting $\{A_i, i = 0, 1, \ldots, 4\}$ into (21).

B. LC-PTS1 METHOD

In the LC-PTS1 method, the metric $Q_{l,n}$ is adopted. Before finding the optimal signal sequence $\hat{s}_l[n]$ for the l-th data block, $Q_{l,n}$ should be calculated for all $-L_g/2 + l\tau N \le n \le L_g/2 + l\tau N$. Then, the samples of which $Q_{l,n}$ is not less than Th_Q are selected as dominant time-domain samples, and Th_Q is a threshold determined by considering the PAPR reduction performance and computational complexity. Let S_{Q_l} represent the index set of dominant time-domain samples for the l-th data block which is defined by

$$S_{Q_l} = \left\{n | Q_{l,n} \ge Th_Q, -L_g/2 + l\tau N \le n \le L_g/2 + l\tau N\right\}. \quad (24)$$

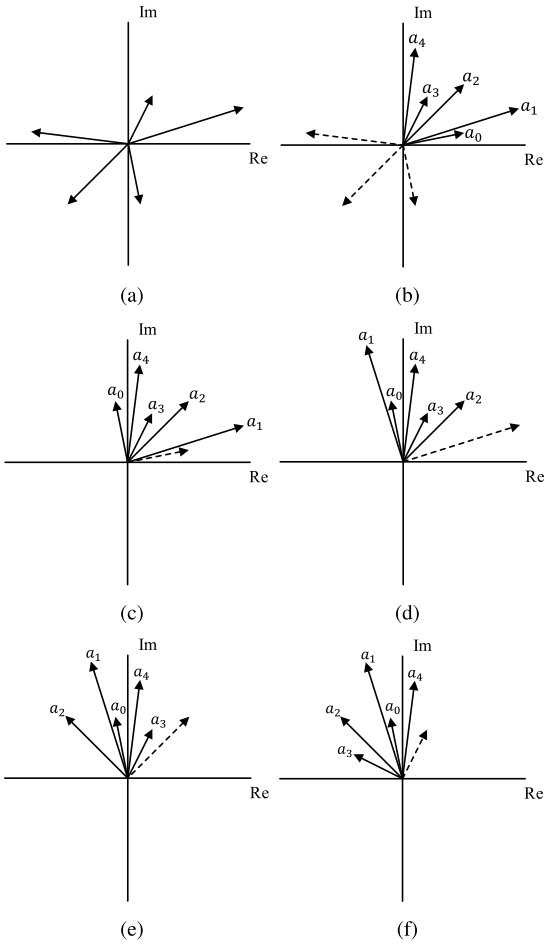

FIGURE 2. The example of new metric.

Next, only the samples $s_l^c[n]$ with $n \in S_{Q_l}$ are generated and used to find the optimal signal sequence. The general procedure of LC-PTS1 method can be formulated by

$$\hat{c} = \arg\min_{c} \max_{n \in S_{Q_l}} \left| \sum_{i=0}^{l-1} \hat{s}_i[n] + s_l^c[n] \right|^2 \tag{25}$$

in which $\hat{c}$ is the index of optimal phase rotation vector. And the integrated optimal signal sequence can be constructed by

$$\hat{s}_l[n] = \sum_{u=0}^{U-1} b_u^{\hat{c}} s_l^{(u)}[n], -L_g/2 + l\tau N \le n \le L_g/2 + l\tau N. \tag{26}$$

Therefore, the LC-PTS1 method can reduce the computational complexity since only a subset time-domain samples in the candidate signal sequences are generated.

C. LC-PTS2 METHOD

In the LC-PTS1 method, the threshold Th_Q is utilized to select the dominant time-domain samples. Note that a trade-off controlled by Th_Q exists between the PAPR reduction performance and the reduction of computational complexity. In order to achieve a low computational complexity, Th_Q will be relatively high. Thus, there may exist some data blocks of which S_{Q_l} are empty. For these data blocks, the original signal sequences without phase rotation are chosen for transmission, i.e.,

$$\hat{s}_l[n] = \sum_{u=0}^{U-1} s_l^{(u)}[n]. \tag{27}$$

Although the emptying of S_{Q_l} ensures that the original signal sequence has no high power sample, the phase rotation can still reduce peak power of signal sequence in most cases. In consideration of the interference that current signal sequence brings to next signal sequence, a lower PAPR signal sequence can be helpful to the next signal sequence in achieving lower PAPR.

On the other hand, there also exist some data blocks of which size of S_{Q_l} are large. For these data blocks, using overmuch dominant time-domain samples is not cost-effective in terms of the PAPR reduction improvement. Thus, reducing the number of dominant time-domain samples and diverting them to the data blocks of which the size of S_{Q_l} are small or even empty is a good way to improve the PAPR reduction performance.

According to the analysis above, we propose the LC-PTS2 method. Same as the LC-PTS1 method, in the l-th data block, we first calculate $Q_{l,n}$ for all $-L_g/2+l\tau N \le n \le L_g/2+l\tau N$. After that, all $Q_{l,n}$ in l-th data block are ranked in descending order and the samples corresponding to the first p $Q_{l,n}$ are chosen as dominant time-domain samples. Let P_{Q_l} represent the p-th largest $Q_{l,n}$. The index set of dominant time-domain samples for the l-th data block can be defined by

$$P_{Q_l} = \left\{ n | Q_{l,n} \ge P_{Q_l}, -L_g/2 + l\tau N \le n \le L_g/2 + l\tau N \right\}. \tag{28}$$

Compared with a fixed threshold Th_Q in LC-PTS1 method, in LC-PTS2 method, the threshold is changed and the size of index set is constant p for different l.

Then, the samples $s_l^c[n]$ with $n \in P_{Q_l}$ are generated and used in finding the optimal signal sequence. Finally, the general procedure of LC-PTS2 method can be formulated by

$$\hat{c} = \arg\min_{c} \max_{n \in P_{Q_l}} \left| \sum_{i=0}^{l-1} \hat{s}_i[n] + s_l^c[n] \right|^2, \tag{29}$$

and the integrated optimal signal sequence can also be constructed by (26).

V. PEAK DISTRIBUTION AND SAMPLE REMOVING

It has been mentioned in section II that a T-orthogonal shaping pulse is employed in MFTN signaling. Without loss of generality, RRC pulse is adopted in the following analysis. For a sampled RRC pulse $g[n]$, the amplitude is not constant with different index n, which will influence the position distribution of the sample with peak power.

As an example, Fig. 3 exhibits the power of MFTN signal sequence under different time index n, in which the number

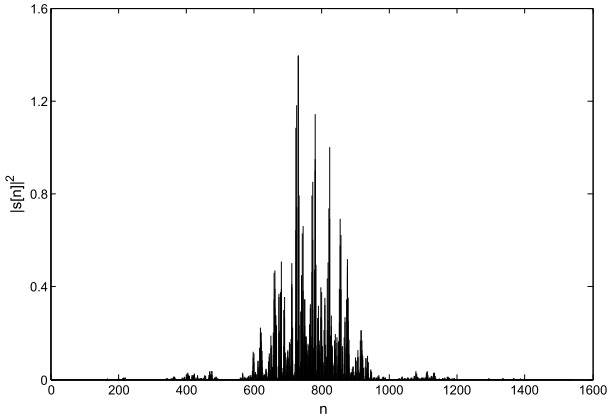

FIGURE 3. An example of MFTN signal sequence.

of subcarriers is $K = 64$, shaping pulse is RRC pulse with $\beta = 0.3$ and frequency packing factor is $\upsilon = 0.5$. Obviously, the samples with high power are comparatively concentrated on the middle part of signal sequence corresponding to the part of RRC pulse $g[n]$ with high amplitude. It is reasonable for us to conjecture that there is a higher probability for sample with peak power to be located in the middle part of the signal sequence.

In order to confirm our conjecture, some additional computer simulations are employed here to acquire the statistical position distribution of peak power sample in the signal sequence. In consideration of the fact that the methods proposed in this paper take the previous symbols into account and the utilization of position distribution in these methods, the influences of previous MFTN symbols are considered when acquiring the statistical position distribution. Concretely, we acquire the position distribution of peak power sample in the sequence expressed by

$$\sum_{i=0}^{l-1} \hat{s}_i[n] + s_l[n], -L_g/2 + l\tau N \le n \le L_g/2 + l\tau N \quad (30)$$

in which $\hat{s}_i[n]$ is previous MFTN signal sequences processed by PTS-AS method and $s_l[n]$ is the randomly generated original signal sequence.

In the additional simulations, the number of subcarriers is $K = 64$, RRC pulse with $\beta = 0.3$ and $L_g = 6N$ is employed, and $W = 4$ and $U = 4$ are employed in the PTS-AS method. We segment the sequence in (30) into 10 equal length intervals, and gather the statistical probability of peak power sample being located in each interval. Fig. 4(a) shows the position distribution of peak power sample in MFTN signal sequence with $\tau = 0.5$ and $\upsilon = 0.5$. Obviously, the sample with peak power tends to be located in the middle part of the signal sequence. Moreover, the position distribution in MFTN signal sequence with $\tau = 0.8$ and $\upsilon = 0.8$ is shown in Fig. 4(b). We can see that the characteristic of position distribution still holds.

Since that the sample with peak power tends to be located in the middle part of the signal sequence, there are some

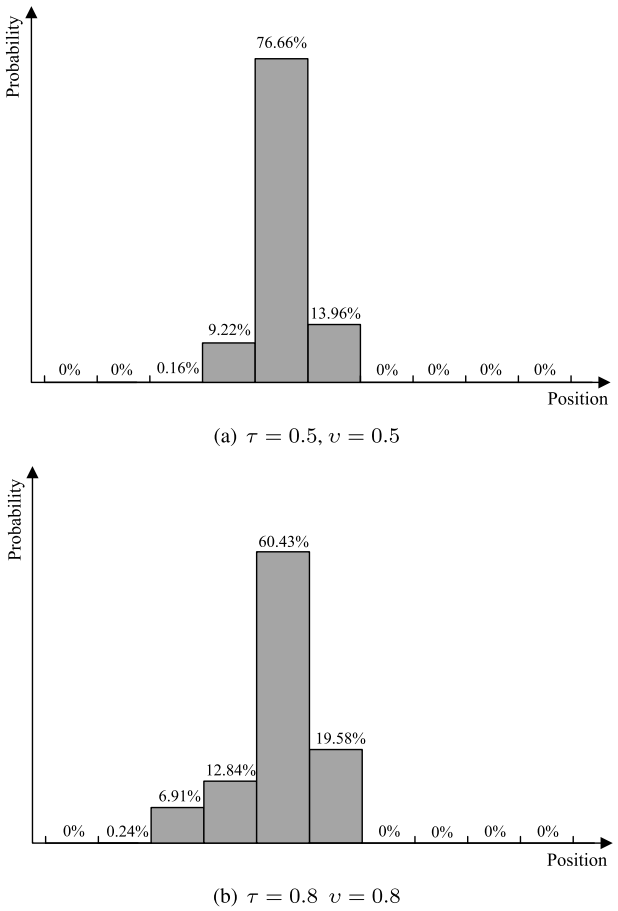

FIGURE 4. Position distribution of sample with peak power.

intervals which have almost no possibility for the appearance of sample with peak power. We can remove the samples in these intervals from the calculation of new metric by directly setting $Q_{l,n} = 0$ without degrading the PAPR reduction performance. And it can effectively reduce the computational complexity in the calculation of new metric. Although the analysis and the simulations above are based on RRC pulse, they can be easily extended to other pulses which means that the sample removing is widely applicable. Moreover, we can segment the sequence into more intervals to make the sample removing more precise.

VI. PERFORMANCE ANALYSIS

In this section, we analyze the performance of proposed methods in this paper, i.e., PTS-AS, LC-PTS1, LC-PTS2. The computational complexity of the proposed PTS schemes are listed and compared. In addition, the computational complexity of LC-PTS2 method combined with sample removing is evaluated and compared. After that, the PAPR reduction performance of these methods are evaluated by computer simulations.

A. COMPUTATIONAL COMPLEXITY

In order to compare the computational complexity of the PTS-AS, LC-PTS1, LC-PTS2, and LC-PTS2 combined with

sample removing, there are three ratio needed to be defined first. For the LC-PTS1 method, the ratio η_1 is defined as the ratio between the expectation number of selected dominant time-domain samples and the number of total signal sequence samples, i.e.,

$$\eta_1 = \frac{E[card(S_{Q_l})]}{L_g + 1} \tag{31}$$

in which $card(\cdot)$ is the extraction of the cardinal number, and $E[\cdot]$ is the expectation operation. For the LC-PTS2 method, the ratio η_2 is defined as the ratio between the number of selected dominant time-domain samples and the number of total signal sequence samples, that is,

$$\eta_2 = \frac{p}{L_g + 1}. \tag{32}$$

Moreover, the ratio η_s is defined as the ratio between number of samples not removed from the calculation of new metric and the number of total signal sequence samples.

Note that the generation of signal subsequence is same for all methods in this paper, the computational complexity analysis in this subsection only focuses on the computational complexity after the generation of subsequences.

For PTS-AS method, there are $U(L_g+1)$ complex additions and $U(L_g + 1)$ complex multiplications in the generation of a candidate signal sequence according to (12). Note that there are C candidate signal sequences, the total numbers of complex additions and complex multiplications are both $CU(L_g + 1)$. For LC-PTS1 and LC-PTS2 method, both $3U(L_g+1)$ complex additions and $(2U+1)(L_g+1)$ complex multiplications are performed in the calculation of new metric $Q_{l,n}$ according to (20), (21) and (23). Then, since only the selected samples of candidate signal sequences are generated for finding the optimal signal sequence by (25) and (29), different from PTS-AS method, both the numbers of complex additions and complex multiplications are $CU\eta_1(L_g + 1)$ or $CU\eta_2(L_g + 1)$ for LC-PTS1 or LC-PTS2. After finding the optimal sequence sequence, $U(L_g + 1)$ complex additions and $U(L_g + 1)$ complex multiplications are needed for constructing the integrated optimal signal sequence by (26) in LC-PTS1 or LC-PTS2 method. For LC-PTS2 method with sample removing, the $Q_{l,n}$ are calculated for part of the samples. Thus, only $3U\eta_s(L_g + 1)$ complex additions and $(2U + 1)\eta_s(L_g + 1)$ complex multiplications are performed for calculating the new metric.

By summarizing the analysis above, we can give the Table 1 which compares the computational complexity of the PTS-AS, LC-PTS1, LC-PTS2, and LC-PTS2 combined with sample removing.

B. SIMULATION RESULTS

In this subsection, we evaluate the accuracy performance of the new metric and PAPR reduction performance of PTS-AS, LC-PTS1, LC-PTS2 and LC-PTS2 with sample removing in MFTN signaling through computer simulation. The subcarriers number $K = 64$ is employed. The oversampling factor is $J = 4$. And the shaping pulse is RRC pulse of which the roll-off factor is $\beta = 0.3$ and the pulse length is $L_g = 6N$.

TABLE 1. Computational complexity after generation of signal subsequences.

(a)

Methods	Number of complex additions
PTS-AS	$CU(L_g + 1)$
LC-PTS1	$(C\eta_1 + 4)U(L_g + 1)$
LC-PTS2	$(C\eta_2 + 4)U(L_g + 1)$
LC-PTS2 with sample removing	$(C\eta_2 + 3\eta_s + 1)U(L_g + 1)$

(b)

Methods	Number of complex multiplications
PTS-AS	$CU(L_g + 1)$
LC-PTS1	$(CU\eta_1 + 3U + 1)(L_g + 1)$
LC-PTS2	$(CU\eta_2 + 3U + 1)(L_g + 1)$
LC-PTS2 with sample removing	$(CU\eta_2 + U + 2U\eta_s + \eta_s)(L_g + 1)$

TABLE 2. Accuracy Performance of $Q_{l,n}$ for Estimation of $M_{l,n}$.

Packing factors	Estimation error rate			
	$U = 4$		$U = 8$	
	$W = 2$	$W = 4$	$W = 2$	$W = 4$
$\tau = 0.5, \upsilon = 0.5$	0%	0%	0%	0%
$\tau = 0.8, \upsilon = 0.8$	0%	0%	0%	0%

Table 2 shows how accurately $Q_{l,n}$ can estimate the value of $M_{l,n}$ where MFTN signaling with $U = 4, 8$, $W = 2, 4$, $\tau = 0.5, 0.8$ and $\upsilon = 0.5, 0.8$ are considered. In the table, the estimation error rate is defined as the ratio between the number of samples with an estimation error of $M_{l,n}$ and the total number of samples. Obviously, the new metric $Q_{l,n}$ can achieve the entirely accurate estimation of $M_{l,n}$. Fig. 5 exhibits the influence of packing factors on the accuracy performance of $Q_{l,n}$. In Fig. 5, W is fixed to 4, and both time and frequency packing factor are started at 0.5 and ended at 0.8 with step 0.1. Even the packing factors vary, $Q_{l,n}$ can keep the accurate estimation of $M_{l,n}$ which indicates that $Q_{l,n}$ has good robustness to the variation of packing factors.

Fig. 6 and Fig. 7 exhibit the PAPR reduction performance of PTS-AS, LC-PTS1 and LC-PTS2 in MFTN signaling with QPSK. The PAPR distribution of original MFTN signaling and conventional PTS method are also shown for comparison. The number of subblocks $U = 4$ and the number of rotation phases $W = 4$ are adopted in all the methods. In these figures, both original MFTN signaling and conventional PTS method have high PAPR which illustrates the poor PAPR reduction performance of conventional PTS method. By taking the previous MFTN symbols into account, the PTS-AS

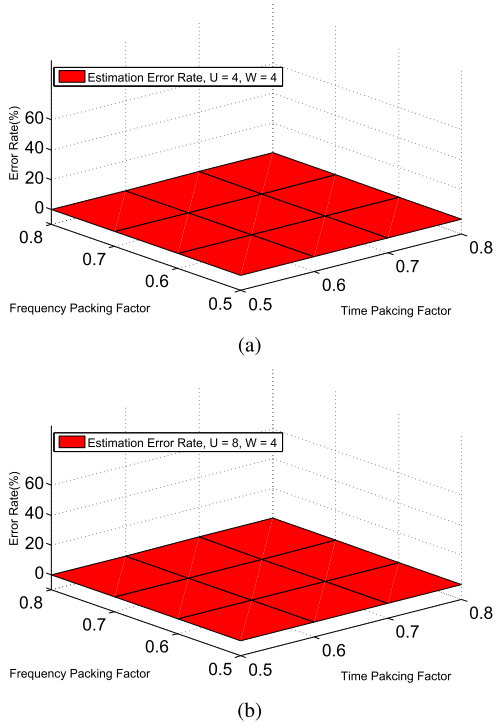

FIGURE 5. The accuracy performance of $Q_{l,n}$.

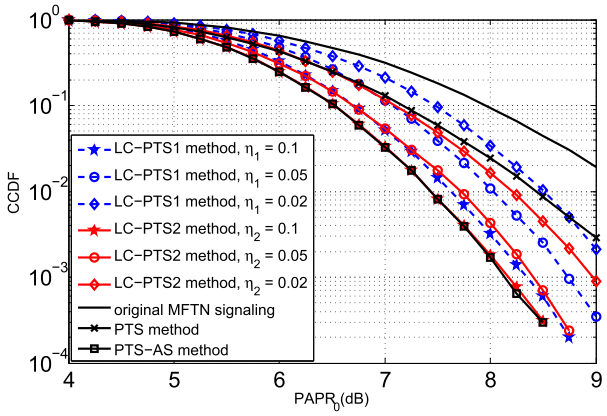

FIGURE 6. PAPR reduction performance in MFTN signaling with QPSK. In this figure, time and frequency packing factors are fixed to $\tau = 0.5$, $\upsilon = 0.5$.

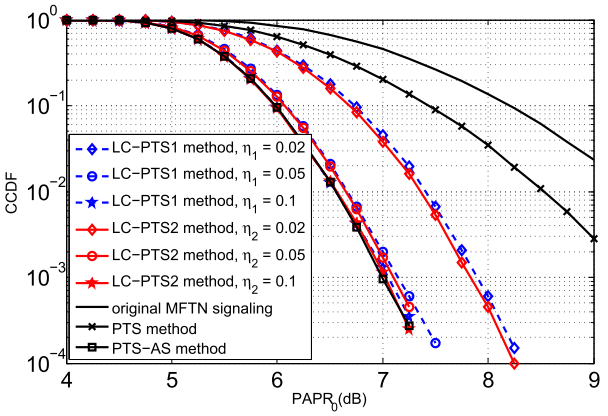

FIGURE 7. PAPR reduction performance in MFTN signaling with QPSK. In this figure, time and frequency packing factors are fixed to $\tau = 0.8$, $\upsilon = 0.8$.

TABLE 3. Numerical computational complexity based on simulation parameters.

(a)

Methods	η_1 / η_2	Complex additions	Complex multiplications
PTS-AS	/	1573888	1573888
LC-PTS1	0.1	182288	177677
	0.05	103440	98829
	0.02	56336	51725
LC-PTS2	0.1	182288	177677
	0.05	103440	98829
	0.02	56336	51725

(b)

Methods	η_s	Complex additions	Complex multiplications
LC-PTS2	/	18444	13833
LC-PTS2 with sample removing	0.4	7380	5535
	0.5	9228	6921

method can overcome the overlapped structure effectively and achieve much better performance than conventional PTS method. In Fig. 6, LC-PTS2 method always shows better performance than LC-PTS1 method when $\eta_1 = \eta_2 = 0.02$, $\eta_1 = \eta_2 = 0.05$ and $\eta_1 = \eta_2 = 0.1$. In Fig. 7, the performance improvement of LC-PTS2 method is not as conspicuous as that in Fig. 6. This confirms the analysis in section IV that a lower PAPR signal sequence can be helpful to the next signal sequence in achieving lower PAPR especially when the interference is serious. According to Table 1, we can quantify the computational complexity and arrive at Table 3(a). When $\eta_1 = 0.1$ and $\eta_2 = 0.1$, both LC-PTS1 and LC-PTS2 only require 11.58% number of complex additions and 11.29% number of complex multiplications of PTS-AS method. When $\eta_1 = 0.05$ and $\eta_2 = 0.05$, the computational complexity can be still reduced, but in cost of performance deterioration, and both LC-PTS1 and LC-PTS2 only require 6.57% number of complex additions and 6.28% number of complex multiplications of PTS-AS method. When $\eta_1 = 0.02$ and $\eta_2 = 0.02$, these two ratios will be reduced to 3.58% and 3.29%. Moreover, the performance of LC-PTS2 method with $\eta_2 = 0.1$ is same as PTS-AS method, which means using dominant time-domain samples can effectively reduce computational complexity without degrading the PAPR reduction performance.

In Fig. 8 and Fig. 9, the performance of LC-PTS2 method and LC-PTS2 combined with sample removing are compared. The signal sequence is segmented into 10 intervals and the analysis in section V is utilized in the simulations. In Fig. 8, the samples in the first two intervals and the last four

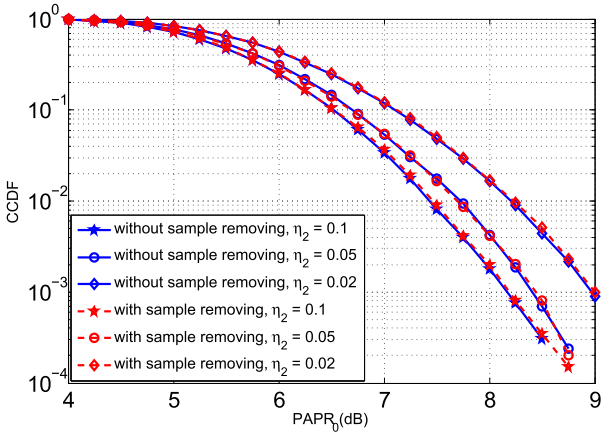

FIGURE 8. PAPR reduction performance of LC-PTS2 method in MFTN signaling with QPSK. In this figure, time and frequency packing factors are fixed to $\tau = 0.5$, $\upsilon = 0.5$.

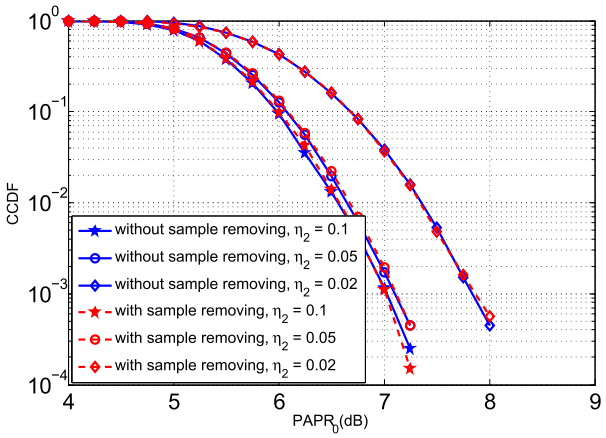

FIGURE 9. PAPR reduction performance of LC-PTS2 method in MFTN signaling with QPSK. In this figure, time and frequency packing factors are fixed to $\tau = 0.8$, $\upsilon = 0.8$.

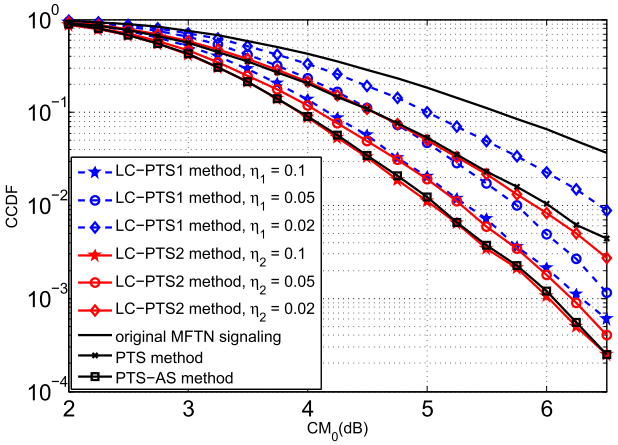

FIGURE 10. CCDF of CM in MFTN signaling with QPSK. In this figure, time and frequency packing factors are fixed to $\tau = 0.5$, $\upsilon = 0.5$.

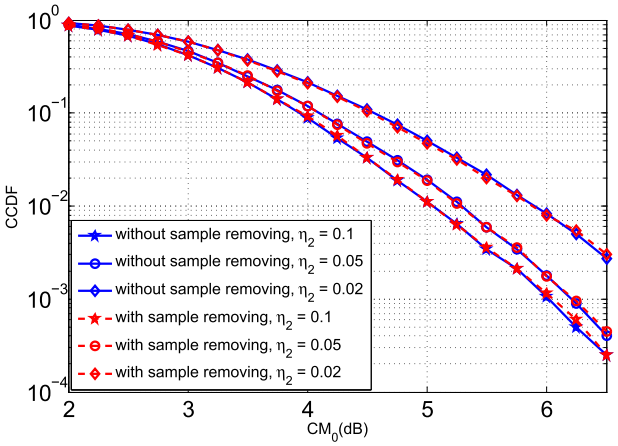

FIGURE 11. CCDF of CM for LC-PTS2 method in MFTN signaling with QPSK. In this figure, time and frequency packing factors are fixed to $\tau = 0.5$, $\upsilon = 0.5$.

intervals are removed from the calculation of $Q_{l,n}$ in the LC-PTS2 method with sample removing. In Fig. 9, the samples in the first interval and the last four intervals are removed. For LC-PTS2 method with sample removing, the η_s in Fig. 8 and Fig. 9 are 0.4 and 0.5, respectively. In Fig. 8, only 40% complex additions and complex multiplications for calculating the $Q_{l,n}$ in LC-PTS2 method are required in LC-PTS2 method with sample removing. And in Fig. 9, this ratio is 50%. The comparison of numerical complexity in calculating the metric is shown in Table 3(b). Even many samples are removed from the calculation of the metric, LC-PTS2 with sample removing always achieves the same performance as LC-PTS2 method which means that sample removing can further reduce the computation complexity.

In recent years, the cubic metric (CM) has been adopted by 3GPP in predicting the amplifier power de-rating [38]. Since the third order intermodulation is the main reason that results in the deterioration of adjacent channel leakage ratio, CM is more accurate in predicting the power de-rating and more related to the amount of distortion induced by nonlinear HPA than PAPR. The CM in the l-th symbol interval is defined as

$$CM_l = \frac{20\log_{10}\left[\sqrt{\frac{\sum_{n=l\tau N}^{(l+1)\tau N}[s[n]]^6}{\tau N P_{av}{}^3}}\right] - 1.52}{1.56} \tag{33}$$

in which $P_{av} = \frac{\sum_{n=l\tau N}^{(l+1)\tau N}[s[n]]^2}{\tau N}$. And the corresponding CCDF is expressed as

$$CCDF = Pr(CM > CM_0). \tag{34}$$

Fig. 10 shows the CCDF of CM in MFTN signaling with QPSK, and Fig. 11 exhibits the CCDF of CM for LC-PTS2 method in MFTN signaling. The results are similar to Fig. 6 and Fig. 8, which proves effectiveness of the proposed methods once again.

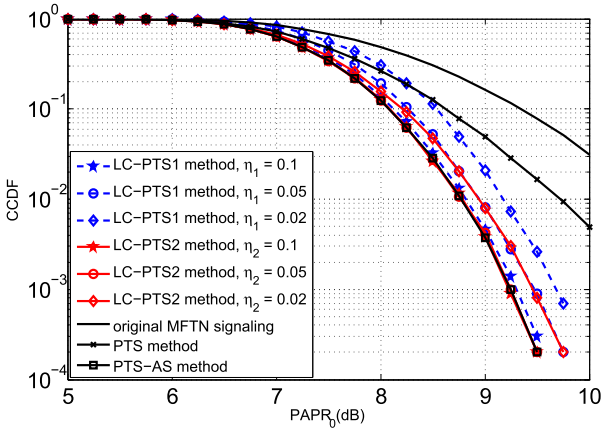

FIGURE 12. PAPR reduction performance in MFTN signaling with QPSK and $K = 256$. In this figure, time and frequency packing factors are fixed to $\tau = 0.5$, $\upsilon = 0.5$.

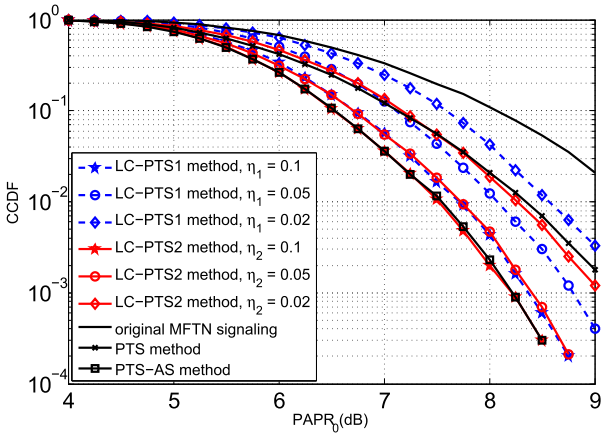

FIGURE 13. PAPR reduction performance in MFTN signaling with QPSK and $\beta = 0.5$. In this figure, time and frequency packing factors are fixed to $\tau = 0.5$, $\upsilon = 0.5$.

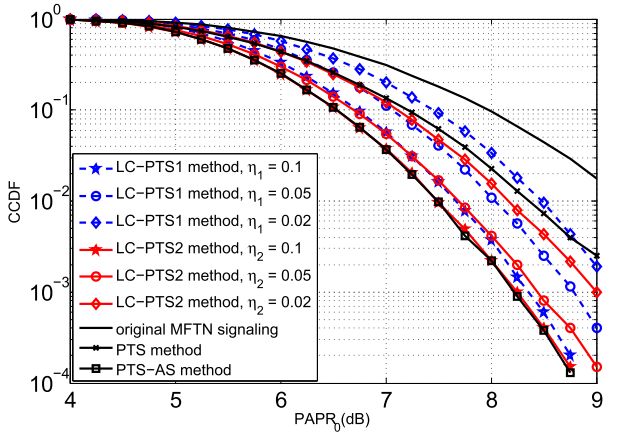

FIGURE 14. PAPR reduction performance in MFTN signaling with 16QAM. In this figure, time and frequency packing factors are fixed to $\tau = 0.5$, $\upsilon = 0.5$.

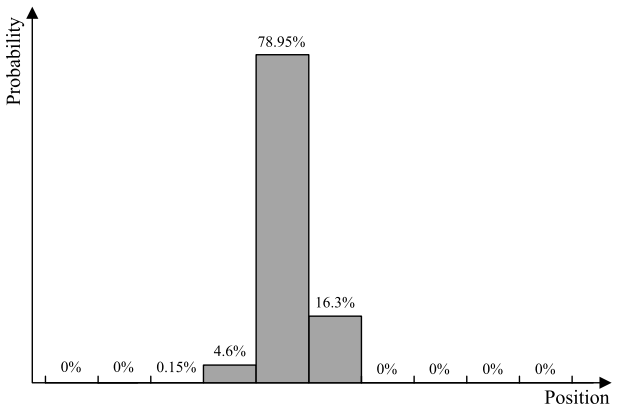

FIGURE 15. Position distribution of sample with peak power in MFTN signaling with 16QAM, $\tau = 0.5$, $\upsilon = 0.5$.

In order to testify that the proposed methods in the paper are generally applicable in MFTN signaling, we also give the performance of them in MFTN signaling with $K = 256$ and $\beta = 0.5$. In Fig. 12, the subcarriers number is $K = 256$. The LC-PTS2 method always shows better performance than LC-PTS1 method when η_1 and η_2 are the same. Moreover, both LC-PTS2 method with $\eta_2 = 0.1$ and $\eta_2 = 0.05$ can achieve the same performance as PTS-AS method and show better performance than LC-PTS1 with $\eta_1 = 0.1$. It means that LC-PTS2 are more superior than LC-PTS1 when K is large. In Fig. 13, the roll-off factor β is fixed to 0.5. Since the ISI is inevitable in MFTN signaling even the β is larger, the simulation result is similar to Fig. 6.

In section II, MFTN signaling with QPSK is utilized as an example to acquire the expression of MFTN signaling and corresponding PAPR. However, there is no limit in the derivation and analysis in section III, IV and V on the modulation order adopted in MFTN signaling. Thus, all the methods proposed in this paper can be easily extended to other high order modulations, e.g, 16QAM. Fig. 14 exhibits the PAPR reduction performance of PTS-AS, LC-PTS1 and LC-PTS2 in MFTN signaling with 16QAM. Both $U = 4$ and $W = 4$ are adopted in all methods. The simulation results in Fig. 14 are similar to that of Fig. 6 and 7, which means the proposed methods are applicable to high order modulations.

In order to acquire the performance of LC-PTS2 with sample removing in MFTN signaling with 16QAM, the position distribution of peak power sample is obtained by computer simulation, which is shown in Fig. 15. Then, by removing the samples in the first two intervals and the last four intervals from the calculation of $Q_{l,n}$, the performance shown in Fig. 16 is acquired. The performance of LC-PTS2 method is also shown for comparison. And the LC-PTS2 with sample removing can achieve the same performance to LC-PTS2 method.

In Fig. 17, the bit error rate (BER) performance of MFTN signaling with QPSK is exhibited. The detection algorithm in [1] is employed here, in which the successive interference cancelation (SIC) is adopted to eliminate the ICI and the BCJR algorithm is adopted to eliminate the ISI. The (7,5) convolutional code is employed as outer code. The iterations

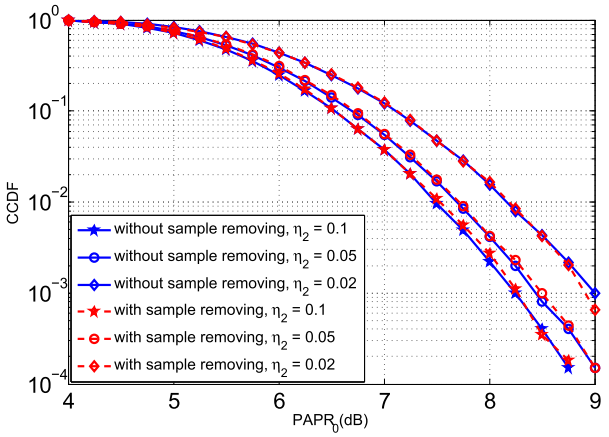

FIGURE 16. PAPR reduction performance of LC-PTS2 method in MFTN signaling with 16QAM. In this figure, time and frequency packing factors are fixed to $\tau = 0.5$, $\upsilon = 0.5$.

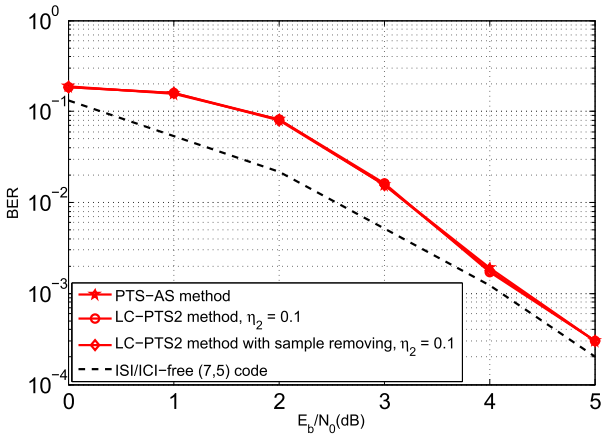

FIGURE 17. BER performance in MFTN signaling with QPSK. In this figure, time and frequency packing factors are fixed to $\tau = 0.8$, $\upsilon = 0.8$.

number of detection algorithm is 7. And we assume that all the side information is received correctly. From Fig. 17, we can see that BER performance of MFTN signaling with PTS-AS, LC-PTS2, LC-PTS2 with sample removing are the same. In fact, these PAPR reduction methods proposed in this paper are only different in the generation of candidate signal sequences and the selection of optimal signal sequence. Once the optimal sequence is found, the integrated optimal signal sequence will be constructed for transmission. In other word, all the proposed PAPR reduction methods are distortionless. Therefore, the simulations results in Fig. 17 are reasonable.

VII. CONCLUSION

The PAPR reduction is an important issue in MFTN signaling. In this paper, we give the expression of MFTN signaling and refine the definition of PAPR. Then, we analyze the poor performance of conventional PTS method and propose PTS-AS method to overcome the overlapped structure in MFTN signaling. After that, a new metric is proposed and shows good accuracy performance. And two low-complexity PTS methods are proposed by using the metric to select dominant time-domain samples. Moreover, by analyzing the position distribution of sample with peak power, some samples are removed in the calculation of metric to further reduce the computational complexity without degrading the PAPR reduction performance.

REFERENCES

[1] F. Rusek and J. B. Anderson, "Multistream faster than Nyquist signaling," *IEEE Trans. Commun.*, vol. 57, no. 5, pp. 1329–1340, May 2009.

[2] Y. Wu and W. Y. Zou, "Orthogonal frequency division multiplexing: A multi-carrier modulation scheme," *IEEE Trans. Consum. Electron.*, vol. 41, no. 3, pp. 392–399, Aug. 1995.

[3] A. Barbieri, D. Fertonani, and G. Colavolpe, "Time-frequency packing for linear modulations: Spectral efficiency and practical detection schemes," *IEEE Trans. Commun.*, vol. 57, no. 10, pp. 2951–2959, Oct. 2009.

[4] A. Piemontese, A. Modenini, G. Colavolpe, and N. S. Alagha, "Improving the spectral efficiency of nonlinear satellite systems through time-frequency packing and advanced receiver processing," *IEEE Trans. Commun.*, vol. 61, no. 8, pp. 3404–3412, May 2013.

[5] T. Delamotte and G. Bauch, "Receiver design for GEO satellite systems using MIMO and time-frequency packing," in *Proc. Int. OFDM Workshop*, Essen, Germany, Aug. 2014, pp. 9–16.

[6] G. Colavolpe and T. Foggi, "Time-frequency packing for high-capacity coherent optical links," *IEEE Trans. Commun.*, vol. 62, no. 8, pp. 2986–2995, Aug. 2014.

[7] J. E. Mazo, "Faster-than-Nyquist signaling," *Bell Syst. Tech. J.*, vol. 54, no. 8, pp. 1451–1462, 1975.

[8] A. D. Liveris and C. N. Georghiades, "Exploiting faster-than-Nyquist signaling," *IEEE Trans. Commun.*, vol. 51, no. 9, pp. 1502–1511, Sep. 2003.

[9] F. Rusek and J. B. Anderson, "The two dimensional Mazo limit," in *Proc. IEEE Int. Symp. Inf. Theory*, Adelaide, SA, Australia, Sep. 2005, pp. 970–974.

[10] S. Peng, A. Liu, H. Fang, K. Wang, and X. Liang, "Turbo frequency domain equalization and detection for multicarrier faster-than-nyquist signaling," in *Proc. Wireless Commun. Netw. Conf. (WCNC)*, Mar. 2017, pp. 1–6.

[11] S. Peng, A. Liu, X. Tong, and K. Wang, "On max-SIR time–frequency packing for multicarrier faster-than-nyquist signaling," *IEEE Commun. Lett.*, vol. 21, no. 10, pp. 2142–2145, Oct. 2017.

[12] F. Schaich and T. Wild, "A reduced complexity receiver for multi-carrier faster-than-Nyquist signaling," in *Proc. IEEE Globecom Workshops*, Dec. 2013, pp. 235–240.

[13] C. Le, M. Schellmann, M. Fuhrwerk, and J. Peissig, "On the practical benefits of faster-than-Nyquist signaling," in *Proc. Int Conf. Adv. Technol.*, Oct. 2015, pp. 208–213.

[14] S. Peng, A. Liu, K. Wang, and X. Liang, "PAPR reduction of multicarrier faster-than-Nyquist signals with partial transmit sequence," *IEEE Access*, vol. 5, pp. 24931–24937, Dec. 2017.

[15] J. C. Chen, "Application of quantum-inspired evolutionary algorithm to reduce PAPR of an OFDM signal using partial transmit sequences technique," *IEEE Trans. Broadcast.*, vol. 56, no. 1, pp. 110–113, Mar. 2010.

[16] Y. Wang, W. Chen, and C. Tellambura, "A PAPR reduction method based on artificial bee colony algorithm for OFDM signals," *IEEE Trans. Wireless Commun.*, vol. 9, no. 10, pp. 2994–2999, Oct. 2010.

[17] N. Taşpınar, A. Kalinli, and M. Yıldırım, "Partial transmit sequences for PAPR reduction using parallel tabu search algorithm in OFDM systems," *IEEE Commun. Lett.*, vol. 15, no. 9, pp. 974–976, Sep. 2011.

[18] J. Zhou, E. Dutkiewicz, R. Liu, X. Huang, G. Fang, and Y. Liu, "A modified shuffled frog leaping algorithm for PAPR reduction in OFDM systems," *IEEE Trans. Broadcast.*, vol. 61, no. 4, pp. 698–709, Dec. 2015.

[19] J. Hou, J. Ge, and J. Li, "Peak-to-average power ratio reduction of OFDM signals using PTS scheme with low computational complexity," *IEEE Trans. Commun.*, vol. 57, no. 1, pp. 143–148, Mar. 2011.

[20] L. Wang and J. Liu, "PAPR reduction of OFDM signals by PTS with grouping and recursive phase weighting methods," *IEEE Trans. Broadcast.*, vol. 57, no. 2, pp. 299–306, Jun. 2011.

[21] X. Qi, Y. Li, and H. Huang, "A low complexity PTS scheme based on tree for PAPR reduction," *IEEE Commun. Lett.*, vol. 16, no. 9, pp. 1486–1488, Sep. 2012.

[22] W. S. Ho, A. S. Madhukumar, and F. Chin, "Peak-to-average power reduction using partial transmit sequences: A suboptimal approach based on dual layered phase sequencing," *IEEE Trans. Broadcast.*, vol. 49, no. 2, pp. 225–231, Jun. 2003.
[23] J. Chen, "Partial transmit sequences for peak-to-average power ratio reduction of OFDM signals with the cross-entropy method," *IEEE Signal Process Lett.*, vol. 16, no. 6, pp. 545–549, Jun. 2009.
[24] Y.-J. Cho, J.-S. No, and D.-J. Shin, "A new low-complexity PTS scheme based on successive local search using sequences," *IEEE Commun. Lett.*, vol. 16, no. 9, pp. 1470–1473, Sep. 2012.
[25] Y. A. Jawhar, L. Audah, M. A. Taher, K. N. Ramli, N. S. M. Shah, M. Musa, and M. S. Ahmed, "A review of partial transmit sequence for PAPR reduction in the OFDM systems," *IEEE Access*, vol. 7, no. 1, pp. 18021–18041, Feb. 2019.
[26] S. Ku, C. Wang, and C. Chen, "A reduced-complexity PTS-based PAPR reduction scheme for OFDM systems," *IEEE Trans. Wireless Commun.*, vol. 9, no. 8, pp. 2455–2460, Aug. 2010.
[27] K.-S. Lee, Y.-J. Cho, J.-Y. Woo, J.-S. No, and D.-J. Shin, "Low-complexity PTS schemes using OFDM signal rotation and pre-exclusion of phase rotating vectors," *IET Commun.*, vol. 10, no. 5, pp. 540–547, 2016.
[28] Y. Cho, K. H. Kim, J. Y. Woo, K. Lee, J. S. No, and D. J. Shin, "Low-complexity PTS schemes using dominant time-domain samples in OFDM systems," *IEEE Trans. Broadcast.*, vol. 63, no. 2, pp. 440–445, Jun. 2017.
[29] K. Lee, H. Kang, and J. No, "New PTS schemes with adaptive selection methods of dominant time-domain samples in OFDM systems," *IEEE Trans. Broadcast.*, vol. 64, no. 3, pp. 747–761, Sep. 2018.
[30] Y. Zhou, T. Jiang, C. Huag, and S. Cui, "Peak-to-average power ratio reduction for OFDM/OQAM signals via alternative-signal method," *IEEE Trans. Veh. Technol.*, vol. 63, no. 1, pp. 494–499, Jan. 2014.
[31] Y. Jawhar, K. Ramli, M. Taher, N. Shah, L. Audah, M. Ahmed, T. Abbas, "New low complexity segmentation scheme of partial transmit sequence technique to reduce the high PAPR value in OFDM systems," *ETRI J.*, vol. 40, pp. 1–15, Aug. 2018.
[32] Y. A. Al-Jawhar, N. S. M. Shah, M. A. Taher, M. S. Ahmed, and K. N. Ramli, "An enhanced partial transmit sequence segmentation schemes to reduce the PAPR in OFDM systems," *Int. J. Adv. Comput. Sci. Appl.*, vol. 7, no. 12, pp. 66–75, 2017.
[33] Y. A. Al-Jawhar, K. N. Ramli, M. S. Ahmed, R. Abdulhasan, H. Farhood, and M. Alwan, "A New Partitioning Scheme for PTS Technique to Improve the PAPR Performance in OFDM Systems," *Int. J. Eng. Technol. Innov.*, vol. 8, no. 3, pp. 217–227, May 2018.
[34] Y. A. Jawhar, R. A. Abdulhasan, and K. N. Ramli, "A new hybrid sub-block partition scheme of PTS technique for reduction PAPR performance in OFDM system," *ARPN J. Eng. Appl. Sci.*, vol. 11, pp. 3904–3910, Apr. 2016.
[35] A. Liu, S. Peng, L. Song, X. Liang, K. Wang, and Q. Zhang, "Peak-to-average power ratio of multicarrier faster-than-nyquist signals: Distribution, optimization and reduction," *IEEE Access*, vol. 6, pp. 11977–11987, 2018.
[36] L. Yang, R. S. Chen, Y. M. Siu, and K. K. Soo, "PAPR reduction of an OFDM signal by use of PTS with low computational complexity," *IEEE Trans. Broadcast.*, vol. 52, no. 1, pp. 83–86, Mar. 2006.
[37] Y. Xiao, X. Lei, Q. Wen, and S. Li, "A class of low complexity PTS techniques for PAPR reduction in OFDM systems," *IEEE Signal Process. Lett.*, vol. 14, no. 10, pp. 680–683, Oct. 2007.
[38] *Cubic Metric in 3GPP-LTE*. document R1-060023, Jan. 2006.

BIAO CAI received the B.S. degree in communication engineering and the M.S. degree in communications and information system from the College of Communications Engineering, PLA University of Science and Technology, Nanjing, China, in 2014 and 2017, respectively. He is currently pursuing the Ph.D. degree in communications and information system with the College of Communications Engineering, PLA Army Engineering University.

His research interests mainly include satellite communication, channel estimation, and signal processing.

AIJUN LIU received the B.S. degree in microwave communications and the M.S. and Ph.D. degrees in communications engineering and information systems from the College of Communications Engineering, PLA Army Engineering University, Nanjing, China, in 1990, 1994, and 1997, respectively, where he is currently a Full Professor with the College of Communications Engineering.

Since 2015, he has been a Visiting Scholar with the Department of Electrical and Computer Engineering, University of Waterloo, Waterloo, ON, Canada. His current research interests include satellite communication system theory, signal processing, space heterogeneous networks, channel coding, and information theory.

XIAOHU LIANG received the B.S. degree in communication engineering from the School of Communication and Information Engineering, University of Electronic Science and Technology of China, Chengdu, China, in 2011, and the M.S. and Ph.D. degrees in communications and information system from the College of Communications Engineering, PLA University of Science and Technology (PLAUST), Nanjing, China, in 2013 and 2016, respectively.

He is currently a Lecturer with PLA Army Engineering University (PLAAEU). His research interests include satellite communication, signal processing, and information theory.